



ELSEVIER

Colloids and Surfaces

A: Physicochemical and Engineering Aspects 140 (1998) 269–278

COLLOIDS
AND
SURFACES

A

A phenomenological approach to relaxation in disordered systems

P. Codastefano ^a, F. Sciortino ^a, P. Tartaglia ^{a,*}, F. Bordi ^b, A. Di Biasio ^c

^a *Dipartimento di Fisica, Università di Roma La Sapienza and Istituto Nazionale di Fisica della Materia, Unità di Roma La Sapienza, Piazzale Aldo Moro 2, I-00185 Roma, Italy*

^b *Università di Roma Tor Vergata, I-00175 Roma, Italy*

^c *Università di Camerino, I-62032 Camerino, Italy*

Received 10 February 1997; accepted 21 April 1997

Abstract

We propose a phenomenological approach to relaxation in disordered systems which is modelled after the well-known percolation behaviour. The approach shows an interesting behaviour of the time correlation function of relevant variables which is characterized by three temporal regimes, an initial exponential decay, a power-law regime and a stretched exponential decay for long times. We give some relevant examples of this behaviour in a wide variety of systems such as gels, microemulsions and glasses. © 1998 Elsevier Science B.V. All rights reserved.

Keywords: Relaxation; Disordered systems; Complex liquids

1. Introduction

In this paper, we introduce a phenomenological model of relaxation in disordered systems which is inspired by the well-known percolative transition [1]. For our purposes the latter can be considered as based on the self-similarity of the structures formed by the interactions of elementary units, which form clusters characterized by a non-integer fractal dimension. Self-similarity also shows up in the distribution of clusters, which is given by a cut-off limited power-law as well. Fig. 1 shows a typical example of percolation clusters on a two-dimensional discrete lattice, observed on increasingly smaller length scales in order to show their self-similarity. Assuming that these clusters are independently relaxing units, we will be able to define two well-separated time scales which define

three different behaviours for the time correlation function of some selected variable.

In order to illustrate the common features of relaxation in disordered systems, we select some typical examples that we will treat in more detail in the following sections. Fig. 2 shows the time correlation function of the density fluctuations of the light quasi-elastically scattered by a sol on approaching the gel transition. It is apparent that the curves tend to behave more and more as a power-law when approaching the gelation threshold. In a microemulsion, close to a critical miscibility point [2] the same quantity instead shows a wide region where a typical stretched exponential behaviour arises and characterizes the slow decay of the spectra, as shown in Fig. 3. A similar behaviour can be observed in the frequency domain, e.g. in the case of dielectric relaxation in microemulsions close to a percolation threshold [3]. In this case, a power-law expression in fre-

* Corresponding author.

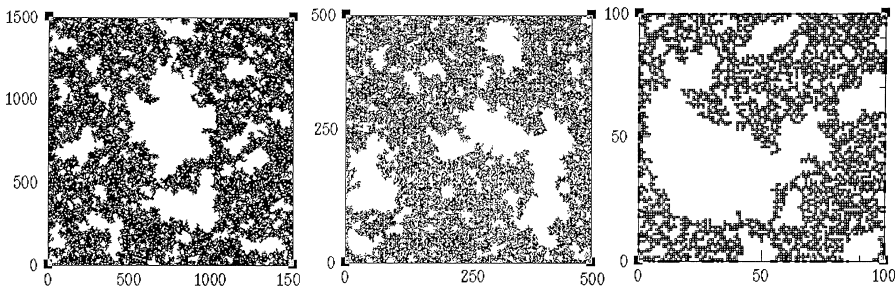


Fig. 1. Percolation clusters on a two-dimensional discrete lattice observed on increasingly smaller length scales in order to show their self similarity.

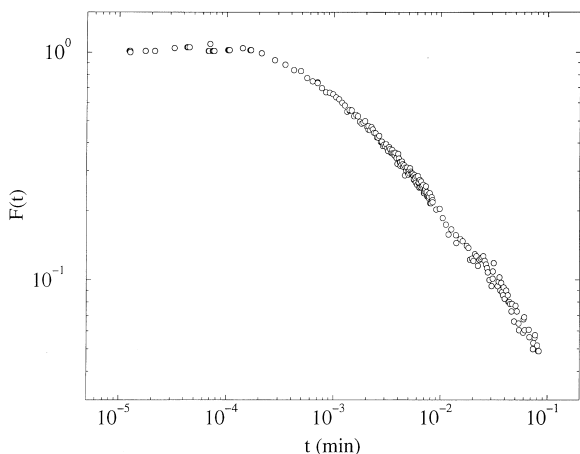


Fig. 2. The density time correlation function for a sol close to the gel transition.

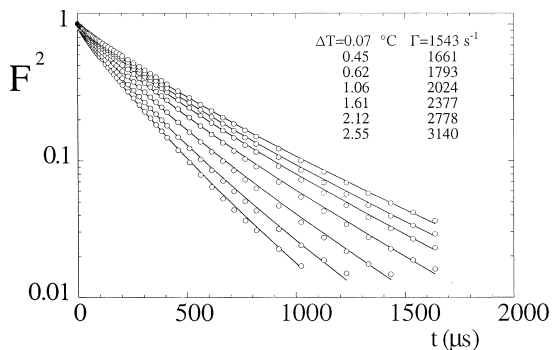


Fig. 3. The concentration time correlation function in a microemulsion close to a critical point: ΔT is the temperature distance from the critical point and Γ is the linewidth.

quency describes the relaxation in the vicinity of the relaxation frequency [4] as shown in Fig. 4.

In Section 2 we introduce a phenomenological

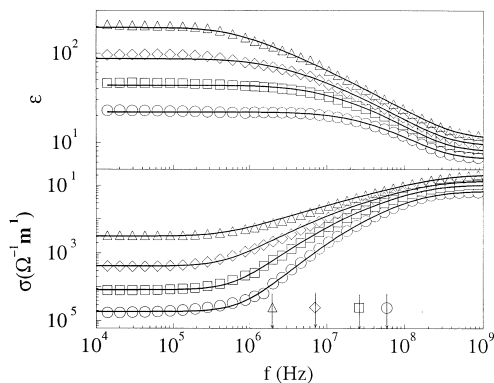


Fig. 4. Conductivity and permittivity relaxation in a three-component microemulsion close to a percolation threshold.

theory, while in Section 3 we describe light scattering measurements on a gel-forming sol. In Section 4, we apply these concepts to microemulsion systems, and finally, in Section 5, we consider the approach to the glass transition of supercooled liquids as described by the mode-coupling theory.

2. Theory

In order to start with a simple case, we assume the system to be made of independent physical clusters generated by aggregation of smaller units due to an attractive interaction. This is the case of sol particles at gelation or microemulsion systems close to percolation, where the elementary units are surfactant coated water droplets, amongst which a short-ranged attractive potential has been shown to act. We note that in a real system, the

clusters are not always independent and the ones that have this property may vary according to the probe that is used to detect them. This fact is particularly evident in the case of percolation, where it has been shown that while conductivity measurements really detect the nearest-neighbour clusters made of touching particles, quasi-elastic scattering experiments observe different objects, i.e. dilute clusters where some of the bonds between the particles are broken. This situation has been demonstrated in the case of lattice systems at criticality, where clusters have been shown to coincide with the critical ones and to percolate exactly at the critical point [5]. In general, we will assume that it is always possible using an appropriate transformation of variables to divide the system in smaller subsystems of independent entities we will call modes.

The assumption of simple exponential relaxation of the independent modes gives the time correlation function $F_k(t)$ for the k th mode

$$F_k(t) = A_k e^{-t/\tau_k}, \tag{1}$$

where the relaxation amplitude A_k and the relaxation time τ_k are both assumed to be power laws of the variable k

$$A_k \sim k^{\alpha+\sigma}, \quad \tau_k = \tau_1 k^\gamma. \tag{2}$$

where τ_1 is the relaxation time for the fastest mode and the three indices have been introduced for reasons that will become clear shortly. The modes distribution function is also assumed to be a power law:

$$c(k) \sim k^{-\sigma} \exp\left[-\frac{k-1}{k_c}\right], \tag{3}$$

with an upper cut-off introduced in order to have a finite upper relaxation time for the slowest mode of the system. In summary, the correlation function of the whole system will be given by:

$$F(t) = \frac{1}{k_c^{1+\alpha} \Gamma\left(1+\alpha, \frac{1}{k_c}\right)} \times \int_1^\infty dk k^\sigma \exp\left[-\frac{t}{k_c} - \frac{t}{\tau_1} k^{-\gamma}\right]. \tag{4}$$

where the prefactor involves the incomplete gamma function $\Gamma(a, x)$ and ensures the normalization $F(0) = 1$. If we consider systems formed by real clusters, the index k can be identified with the number of units in the cluster itself; in general, k will be used to label the modes of the system. In more transparent physical terms, the correlation function can be expressed as a superposition of relaxation times:

$$F(t) = \int_{\tau_1}^\infty \frac{d\tau}{\tau} g(\tau) \exp\left[-\frac{t}{\tau}\right], \tag{5}$$

where $[g(\tau)]/(\tau)$ is the distribution of times

$$g(\tau) = \frac{1}{\gamma \Gamma\left[1+\alpha, \left(\frac{\tau_c}{\tau_1}\right)^{-1/\gamma}\right]} \times \left(\frac{\tau}{\tau_c}\right)^{1+\alpha/\gamma} \times \exp\left[-\left(\frac{\tau}{\tau_c}\right)^{1/\gamma}\right] \tag{6}$$

and $\tau_c = \tau_1 k_c^\gamma$ defines the cut-off relaxation time. In summary, we obtain an expression of $F(t)$ which involves only the two exponents α and γ and the two relaxation times τ_1 and τ_c , corresponding to the fastest and slowest relaxations in the system. It is interesting to note that while τ_1 is a fixed quantity depending only on the nature of the elementary units of the system, τ_c is a quantity that in general depends on some external driving parameter, like temperature or pressure or time, which allows the scaling regime to become larger and larger. When the upper cut-off time diverges, true scaling is observed. The general form of a power-law distribution of relaxation times with an upper cut-off already appears in some well-known interpolation formula for relaxation, like that of Cole–Davidson [6].

Let us now derive the behaviour of the time correlation function in the three times regimes delimited by the two times τ_1 and τ_c .

(1) $t \ll \tau_1$. For short times, we obtain a linear behaviour different according to the value of the indices. For $1+\alpha < 0$, $F(t)$ is a function of τ_1 only:

$$F(t) \approx 1 + \frac{1+\alpha}{\gamma-1-\alpha} \times \frac{t}{\tau_1}. \tag{7}$$

In the opposite case $1+\alpha>0$, we obtain for $0<\gamma<1+\alpha$ a function of τ_c only:

$$F(t) \approx 1 - \frac{\Gamma(1+\alpha+\gamma)}{\Gamma(1+\alpha)} \times \frac{t}{\tau_c}, \quad (8)$$

while for $0<1+\alpha<\gamma$ we obtain

$$F(t) \approx 1 - \frac{1}{(\gamma-1-\alpha)\Gamma(1+\alpha)} \times \left(\frac{\tau_1}{\tau_c}\right)^{1-\alpha/\gamma} \times \frac{t}{\tau_1}. \quad (9)$$

(2) $\tau_1 \ll t \ll \tau_c$. In the intermediate time regime, the self-similarity of $g(\tau)$ gives a power-law dependence in $F(t)$ in two different ways according to the sign of $1+\alpha$. For $1+\alpha>0$ the quantity $1-F(t)$ behaves as a power-law:

$$F(t) \approx 1 - \frac{\gamma}{(1+\alpha)(\gamma-1-\alpha)} \times \frac{\Gamma\left(2 - \frac{1+\alpha}{\gamma}\right)}{\Gamma(1+\alpha)} \times \left(\frac{t}{\tau_c}\right)^{1+\alpha/\gamma}. \quad (10)$$

For $1+\alpha<0$ we get the true power-law:

$$F(t) \approx -\frac{1+\alpha}{\gamma} \left[\Gamma\left(-\frac{1+\alpha}{\gamma}\right) - \Gamma\left(-\frac{1+\alpha}{\gamma}, \frac{t}{\tau_1}\right) \right] \left(\frac{t}{\tau_1}\right)^{\frac{1+\alpha}{\gamma}}. \quad (11)$$

(3) $t \gg \tau_c$. For long times, $F(t)$ is a stretched exponential decay times a power:

$$F(t) \approx \frac{\sqrt{2\pi/(\gamma+1)}}{\Gamma\left(\alpha+1, \left(\frac{\tau_c}{\tau_1}\right)^{-1/\gamma}\right)} \left(\frac{\gamma t}{\tau_c}\right)^{\alpha+0.5/\gamma+1} \times \exp\left[-\left(\frac{t}{\beta(1-\beta)^{1/\beta-1}\tau_c}\right)^\beta\right], \quad (12)$$

where the universal exponent β is defined as $\beta=1/1+\gamma$. Note that one obtains a pure stretched exponential only when $\alpha=-0.5$ [7].

In summary, we observe a linear (or exponential) initial decay below τ_1 , a scaling behaviour represented by a power law for times above τ_1 and

below τ_c and a rather slowly decaying stretched exponential above τ_c .

3. Gel transition

The sol–gel transition has often been considered as the physical example of a percolation transition. The relaxation can, in fact, be divided into three regimes, an initial exponential decay followed by a power-law and a final slow decay to zero via a stretched exponential. In this case, the driving parameter to the gel transition is time. The closer to the gel point, the more extended is the scaling region described by the power-law. From the microscopic point of view, in branched polymer solutions undergoing aggregation under moderate or aggressive reaction conditions, the collisions between the aggregates may lead to critical clusters growth associated with evolution from sol to gel. During this process, a rich variety of dynamical properties takes place [8,9] and the system exhibits a wide spectrum of independent relaxing modes [10,11].

We performed a set of dynamic light scattering measurements in silica gels obtained from 0.1 M tetramethoxysilicon (TMOS) dispersed in methanol and catalysed by means of 3.0 M H₂O and 0.006 M NH₃OH. The aggregation was controlled by adding to the alcoholic solution an NaCl electrolyte solution of different concentrations from 0.005 to 0.05 M. The analysis of the shape of the spectra, plotted in appropriate scales, shows the three time regimes typical of relaxation in disordered systems. In particular semi-logarithm plots of the correlation functions show the deviation from the simple exponential decay as the reaction yielding the gel transition proceeds. The intermediate times power law is apparent in a double logarithmic plot. When the cluster–cluster aggregation takes place, deviations from an exponential decay become more and more evident. Close to gelation, the decay for the particular system investigated is very slow and at the gel point, at about 908 min, the well-known critical slowing down becomes dominant.

We fitted our measured intensity correlation functions to Eq. (4). Four parameters have to be

determined by the fit, namely k_c , τ_1 , α and γ . In order to establish the value of these parameters, we can take advantage of their different feature and of their physical meaning. So we consider only the parameters k_c and τ_1 as function of aggregation time and assume $\alpha = 1.30 \pm 0.05$ and $\gamma = 1.03 \pm 0.05$. In Fig. 5, some calculated homodyne correlation functions are compared at different times with those observed. As can be seen, the agreement is very good over the whole time interval investigated. Moreover, it must be noted that the curve closest to the gel point (about 908 min) exhibits a power-law dependence in time $\sim t^\phi$ with the exponent $\phi = -0.60 \pm 0.02$, in good agreement with the asymptotic value $2 \times (1 + \alpha)/\gamma = 0.58$ expected from Eq. (11). The parameter τ_1 as a function of different aggregation times is plotted in Fig. 6. A semi-log scale shows, with linear behaviour, the exponential growth occurring at the lowest salt concentration investigated. The time τ_1 describes the fastest mode in the relaxation due to the cooperative diffusion of monomers in solution. This mode behaves independently from the slowest percolative type mode evidenced by very fast increasing of cut-off parameters k_c at times near the gelation and its divergence at gel time t_{gel} . The cut-off k_c in the percolative type mass distribution against the reduced time ϵ exhibits power-law divergence with the exponent $-\nu D = -2.6 \pm 0.1$.

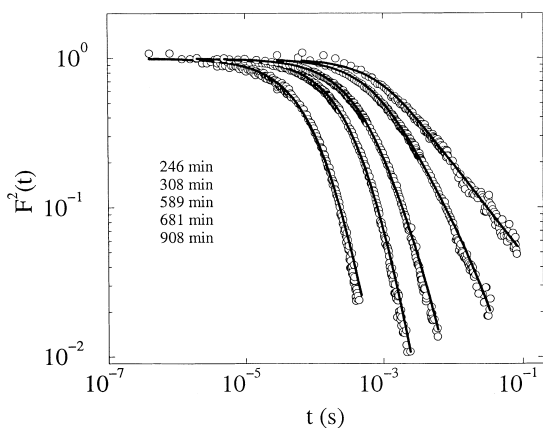


Fig. 5. The squared time density correlation function at different times approaching the gel transition. Note the power-law behaviour as the aggregation time increases.

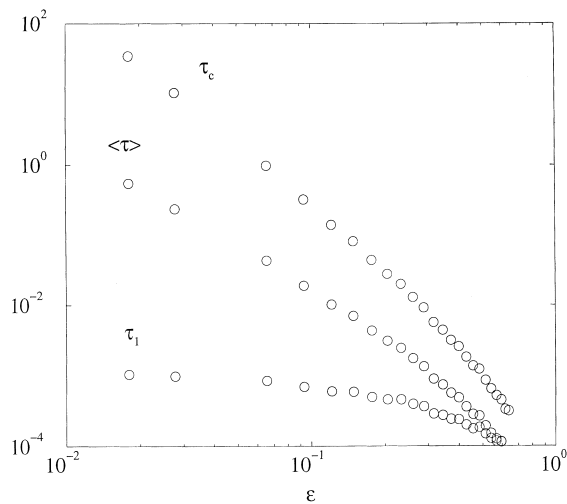


Fig. 6. The smallest timescale τ_1 , the average relaxation time $\langle \tau \rangle$ and the largest timescale τ_c for a sol–gel transition.

The divergence of k_c implies, on the other hand, divergent behaviour in the longest characteristic time $\tau_c = \tau_1 k_c^\gamma$ in the relaxation times distribution, Eq. (6), as well as in the average relaxation time $\langle \tau \rangle$, defined by the expression:

$$\langle \tau \rangle = \int_{\tau_1}^{\infty} d\tau g(\tau) \approx |1 + \alpha| \Gamma(1 + \alpha + \gamma) \tau_1 \times \left(\frac{\tau_c}{\tau_1} \right)^{1 + (1 + \alpha/\gamma)} \quad (13)$$

The characteristic times of the gels we investigated are shown in Fig. 6 and the results can be summarized as follows. The shortest mode in the system, described by the characteristic parameter τ_1 depending on the diffusion of monomers, behaves independently of the percolative mode at the sol–gel transition so when the gelation takes place it does not diverge at gel point. Moreover, the values obtained by fitting the correlation function are in good agreement with those expected from the approximated expression from Eq. (7). The longest mode in the system, described by the characteristic time τ_c depends on the overlapping of branched cluster in the mass percolative type distribution. It manifests an asymptotic behaviour in the pre-gel regime and exhibits a power-law divergence at the gel point, as a function of the

reduced time, like $\sim \epsilon^{-2.6 \pm 0.1}$. The average characteristic time $\langle \tau \rangle$ behaves as τ_c , but diverges against the reduced time as $\sim \epsilon^{-1.8 \pm 0.1}$.

In conclusion, our study has made possible a better understanding of the behaviour of the characteristic times involved in the relaxing modes of the decay of density fluctuations in the region before the gelation and the critical slowing down at the gel point. The asymptotic behaviour of the longest and the average divergent times, as well as the shortest characteristic time, show the goodness of percolative model to fit experimental observation as the percolative transition is approached.

4. Microemulsions

We consider a three-component system made of water, oil (decane) and a surfactant (AOT) which, when the molar ratio of the water to surfactant content $X = [\text{water}]/[\text{surfactant}]$ is constant, has been shown to be formed in some region of the phase diagram by droplets of water separated from the oil phase by a surfactant layer made of amphiphilic molecules. In these regions, the system is effectively a two-component system and can be described using the volume fraction ϕ of the dispersed phase as a thermodynamic variable. The interest in this kind of system derives from the fact that they show a wide variety of behaviours, namely critical miscibility points, loci of percolation points, lamellar phases and bicontinuous phase. For the microemulsion we quoted above, for $X = 40.8$, a critical point exists at a temperature $T \sim 40^\circ\text{C}$ and $\phi \sim 0.10$ and from the vicinity of that point a percolation line extends up to very high volume fractions ($\phi > 0.80$). The measured binodal and percolation lines are shown in Fig. 7 together with the result of the application of a sticky hard sphere model.

We will focus in particular on the percolation line which has been characterized by static electrical conductivity measurements. In fact, this quantity shows a marked increase of several orders of magnitude when approaching a percolation point. The inflection point of the typical sigmoidal curve in a semi-logarithmic scale locates the percolation point. In order to characterize conductivity in this

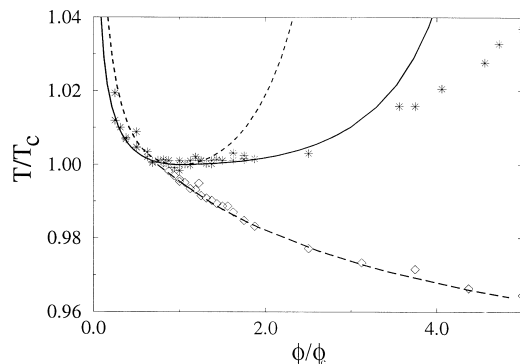


Fig. 7. The measured phase diagram of a water–AOT–decane microemulsion at $X=40.8$. The symbols are the measured values of the binodal and percolation lines, the solid lines refer to a theoretical model of sticky hard spheres. The symbol ϕ refers to the volume fraction of the dispersed phase.

regime, phenomenological power-laws have been used when approaching percolation along a path at constant temperature or at constant volume fraction. Deviations from a power-law are observed close to percolation, where a constant conductivity is measured. A scaling behaviour also exists in the dynamical regime, for example, when measuring the frequency-dependent electrical conductivity since one observes a scaling relationship which involves both the frequency and the distance, in temperature or volume fraction, from percolation. Similar effects are observed for the permittivity of the microemulsion.

The starting point is the calculation of the complex conductivity [12] of a single aggregate by means of an effective medium approximation [13] which gives the correct dependence from the electric parameters of the microemulsion components. The mechanism that even below percolation gives rise to a finite conductivity for the entire system has been identified as anomalous diffusion of the charge carriers in the bulk of a fractal cluster, which grows through the successive aggregation of microemulsion droplets. The result is a conductivity for the single cluster which has the typical form of a single relaxation phenomenon, where the relaxational amplitude and time have the power-law dependence on cluster size, typical of systems with scaling properties. The final step consists of using the appropriate cluster size distri-

bution to account for the polydispersity of the system close to percolation. We consider a matrix of oil, characterized by the conductivity σ_A and permittivity ϵ_A , containing spherical droplets, the electrical parameters of which are σ_B and ϵ_B . Using the effective medium approximation for the complex conductivity of the cluster $\tilde{\sigma}_k = \sigma_k + i\omega\epsilon_k$ in terms of the analogous quantities for the microemulsion components, we obtain:

$$\tilde{\sigma}_k = \tilde{\sigma}_A \frac{A_k \tilde{\sigma}_B + 2\tilde{\sigma}_A}{\tilde{\sigma}_B + B_k \tilde{\sigma}_A} \tag{14}$$

where the quantities A_k and B_k do not depend on the electrical properties of the materials. Eq. (14) can be written in an equivalent way as:

$$\tilde{\sigma}(\omega) = \sigma_{k0} + i\omega \left[\epsilon_{k\infty} + \epsilon_A \frac{\Delta_k}{1 + i\omega\tau_k} \right], \tag{15}$$

where σ_{k0} is the low-frequency conductivity and $\epsilon_{k\infty}$ the high-frequency permittivity. It has the typical form of a single relaxation process with amplitude Δ_k and relaxation time τ_k , two quantities that can be easily related to the parameters A_k and B_k . We use the approximation of conducting clusters in an ideal non-conducting medium since in the case of our system we estimate $\sigma_A \approx 10^{-6} \Omega^{-1} \text{m}^{-1}$, $\epsilon_A \approx 2\epsilon_0$ and $\sigma_B \approx 10^{-2} \Omega^{-1}$, $\epsilon_B \approx 10^2\epsilon_0$, with ϵ_0 being the vacuum permittivity. In this case, the amplitude and the relaxation time for a relaxing cluster of k particles become:

$$\Delta_k^{\text{RC}} = A_k - \frac{2}{B_k}, \quad \tau_k^{\text{RC}} = \frac{\epsilon_A B_k}{\sigma_B}. \tag{16}$$

The two parameters A_k and B_k must then be determined as a function of the number of particles k in a cluster making reference to the physical mechanism of electrical conductivity in microemulsions below the percolation threshold. This mechanism, introduced some time ago by Lagües et al. [14], is known as *stirred percolation* and was studied later on in a more detailed way by Grest et al.[15] and named *dynamic percolation*. The main idea is that once the microemulsion droplets aggregate to form clusters, the charge carriers are capable of moving in the cluster, thus giving rise

to conduction. The motion of the charges in the aggregate is essentially anomalous diffusion on a fractal cluster. The complex frequency-dependent susceptibility of a k -cluster is in general related to the Laplace transform time derivative of the total dipole moment fluctuation $\delta\mu$ time correlation function $\langle \delta\mu(t)\delta\mu(0) \rangle$.

In the RC, limit we can relate the relaxation amplitude Δ_k^{RC} to the static dipole moment correlation function $\langle [\delta\mu(0)]^2 \rangle$ and the relaxation time τ_k^{RC} to its exponential decay constant. Δ_k is related to the product of the mean square charge fluctuations, proportional to the cluster size k and the radius of gyration squared R_k^2 , where $R_k \sim k^{1/D}$ and D is the fractal dimension of the cluster. Consequently Δ_k^{RC} will be proportional to:

$$\Delta_k^{\text{RC}} \approx kR_k^2. \tag{17}$$

If the clusters were compact objects, τ_k^{RC} would be proportional to R_k^2 since the charge carriers perform diffusive motion in the clusters. Since the motion is instead on a fractal aggregate, it is governed by anomalous diffusion and τ_k^{RC} will be related to the radius of gyration through a power which takes into account the anomaly, i.e. the ratio D/\bar{d}

$$\tau_k^{\text{RC}} \approx (R_k^2)^{D/\bar{d}}, \tag{18}$$

where \bar{d} is the so-called spectral exponent. This approximation gives simple expressions for A_k and B_k and as a consequence the complex conductivity of an isolated cluster. Following the analogy with random-bond percolation, we assume that close to the threshold, the number of clusters of size k is given by the typical scaling expression [1] of Eq. (3), characterized by a power-law behaviour and a cut-off cluster size which diverges as the system approaches the percolation threshold. To summarize, we calculate $\tilde{\sigma}$ as a sum of properly weighted independent contributions:

$$\begin{aligned} \tilde{\sigma}(\omega) &= \int_1^\infty dk c(k) \tilde{\sigma}_A \frac{A_k \tilde{\sigma}_B + 2\tilde{\sigma}_A}{\tilde{\sigma}_B + B_k \tilde{\sigma}_A} \\ &= \int_1^\infty dk c(k) \left(\sigma_{k0} + i\omega\epsilon_{k\infty} + \frac{\Delta_k}{1 + i\omega\tau_k} \right). \end{aligned} \tag{19}$$

where Δ_k and τ_k are given by Eqs. (17) and (18), respectively. The previous expressions depends on the materials electrical parameters, two power-law indices and the distance from the percolation threshold, as measured by the cut-off k_c . The latter can then be easily related to a thermodynamic parameter which drives the system to percolation. It can also be shown [12] that Eq. (19) obeys the scaling relations we mentioned in the introduction, both for the static and the frequency-dependent conductivity and permittivity.

We now turn to the comparison with experimental data. Fig. 8 shows the experimentally measured static conductivity as a function of temperature for the system water, decane and AOT in which water has been substituted with brine (see [16]). The solid curve is the theoretical expression in Eq. (19) which gives a power-law behaviour $\sigma_0 \approx |T - T_p|^{s'}$ with $s' = 1.2$ only in a finite T window, not too close to the percolation temperature T_p . In fact, at T_p the conductivity σ_0 reaches a finite value, related to the finite conductivity of the oil phase.

As far as the frequency dependence of the complex conductivity is concerned, Fig. 9 compares theory and experiments in $\epsilon'(\omega)$ and $\epsilon''(\omega)$ for two different volume fractions of the same microemulsion system close to the percolation line [17]. In all cases, the conductivity $\tilde{\sigma}(\omega)$ describes very well, and with the same set of parameters simultaneously, the ω -dependence of σ and ϵ of the

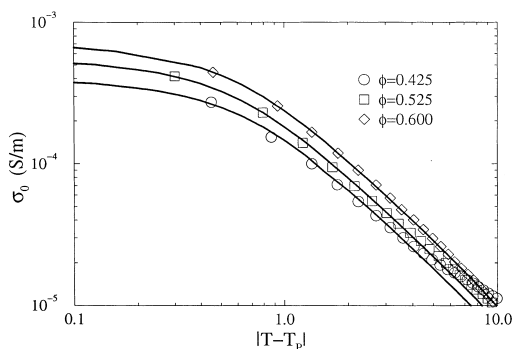


Fig. 8. The static conductivity as a function of temperature for the system water–decane–AOT in which water has been substituted with brine.

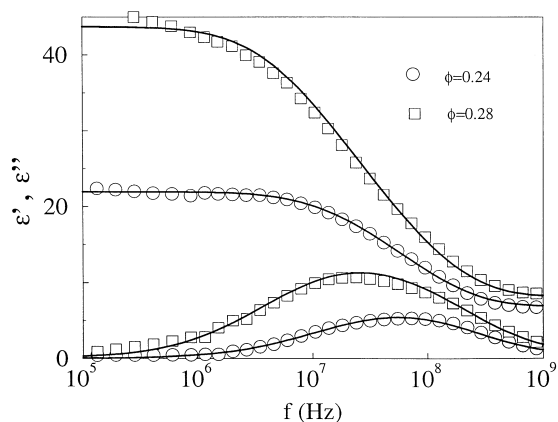


Fig. 9. Relaxation of the real and imaginary part of the permittivity in the system water–decane–AOT.

samples, as well as their limiting zero- and infinite-frequency values.

In conclusion, in order to introduce a quantitative description of the anomalous electric behaviour due to percolation below the threshold, we use a simple model where dynamic percolation is the key ingredient. We assume that the charge carriers that are present due to the ionic nature of the surfactant, perform an anomalous diffusive motion in the bulk of the fractal clusters formed by aggregation of the initial microemulsion droplets and determine in this way the relaxation amplitude and time of a single cluster. In order to do this analytically, we use an effective medium approximation which gives the corrected dependence of the cluster conductivity on the electrical materials parameters. The use of the scaling cluster size distribution to take into account the polydispersity of the microemulsion, gives the final formula of our model, which represents in the frequency domain the general approach we have introduced earlier in the time domain.

5. Glass transition

The glass transition of a supercooled liquid is a subject of considerable interest since a long time. From our point of view, it can be characterized through the behaviour of the time correlation

function of density fluctuations $\phi(t)$. The latter quantity shows, in fact, a rather peculiar behaviour when lowering the temperature. First of all, a two-step relaxation process sets in, with a well-defined separation of time scales. An initial decay can be phenomenologically described by means of a Gaussian approximation, followed by a large plateau region which is approached with a power-law in time and left with a similar law. For longer times, $\phi(t)$ has the typical stretched exponential behaviour of dense complex systems. When in a supercooled state, the correlation function tends to decay to zero for very long times, in contrast to what happens in the glassy states, where a finite value is reached asymptotically in time. This different behaviour marks the so-called ergodic–non-ergodic transition.

A way of describing this phenomenology is provided by the so-called mode-coupling theory for the glass transition [18–20], which is capable of describing the effects we mentioned above not only qualitatively, but with a high degree of quantitative agreement. The final form for the mode-coupling equations in a simple case where the space dependence of the relevant fields is neglected is given by a simple overdamped evolution equation with memory, i.e. a non-local equation with respect to the time dependence. Typically:

$$\frac{d\phi}{dt} + \gamma\phi + \int_0^t dt m(t-t') \frac{d\phi}{dt'} = 0. \quad (20)$$

The memory kernel $m(t)$ is a non-linear functional of the density correlation function itself; one of the simplest cases is given by a linear combination of ϕ and ϕ^2 , the so-called F_{12} model. The kernel also depends on two parameters that are used to locate the glass transition point and the distance from it. The glass transition point is fixed by the situation in which the correlation function is different from zero for times going to infinity. Fig. 10 shows a set of density relaxation curves for this simple model, illustrating the features we just described. Some quantitative features are worth mentioning, especially in the so-called alpha relaxation regime, the one that extends after the plateau.

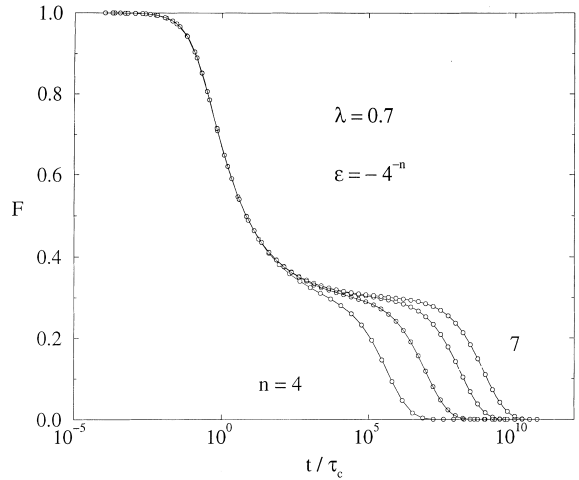


Fig. 10. Density correlation function decay for the F_{12} model of glass transition in the mode-coupling theory. The parameter λ fixes the glass transition point, while ϵ fixes the distance from it.

The behaviour of the density correlations is given by the power-law:

$$\phi(t) \sim t^b, \quad (21)$$

also called the von Schwidler law, when decaying from the constant plateau value. The successive decay is a stretched exponential:

$$\phi(t) \sim e^{-t^3}, \quad (22)$$

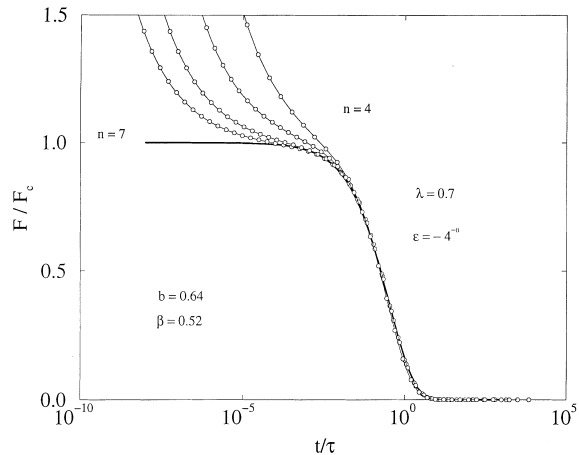


Fig. 11. Time–temperature scaling in the F_{12} model of glass transition.

characterized by an exponent β different from b . In the initial region, a typical time-temperature scaling exists of the form:

$$\phi(t) = t^b F(t/T), \quad (23)$$

where $F(x)$ is a scaling function of the scaled variable involving both time and temperature. We tested whether the power-law and the stretched exponential regime can be described by our phenomenological approach, which qualitatively shows the same features. Motivated by this similarity in the behaviour of $\phi(t)$ as predicted by mode coupling of $\phi(t)$ calculated as sum of independently relaxing modes, we have compared the two curves in Fig. 11. We have used $\gamma=0.92$ and $1+\alpha=0.59$, in agreement with the exponent of the von Schwidler law. In this region of $1+\alpha$, the relevant parameter is τ_c and all curves can be scaled in $t/(\tau_c)$, corresponding to the time-temperature superposition principle [18,19]. The largest relaxation time is identified with the parameter τ_c of our approach. A recent simulation of water in the supercooled regime [21,22] shows the same qualitative and quantitative behaviour we described above and can be equally well described by our approach. Of course, while we are able to also describe the approach to the plateau as well as to predict the value of the exponent in the power-law regime and the scaling behaviour of τ_{glass} from the chosen model, in our case we arbitrarily chose γ and α . This notwithstanding, the agreement is surprisingly good, suggesting that dynamics of the supercooled liquid close to the glass transition is the result of a self-similar distribution of relaxation times.

References

- [1] D. Stauffer, A. Aharony, Introduction to Percolation Theory, Taylor and Francis, London, 1992.
- [2] J. Rouch, P. Tartaglia, S.H. Chen, Phys. Rev. Lett. 71 (1993) 1947.
- [3] C. Cametti, P. Codastefano, P. Taraglia, J. Rouch, S.H. Chen, Phys. Rev. Lett. 64 (1990) 1461.
- [4] C. Cametti, F. Sciortino, P. Tartaglia, J. Rouch, S.H. Chen, Phys. Rev. Lett. 75 (1995) 569.
- [5] A. Coniglio, W. Klein, J. Phys. A 13 (1980) 2775.
- [6] J. Ross MacDonald, Impedance Spectroscopy, Wiley, New York, 1987.
- [7] R. Botet, I.A. Campbell, J.M. Flesselles, R. Jullien, in: R. Jullien, L. Peliti, R. Rammal, N. Boccaro (Eds.), Universalities in Condensed Matter, Springer, Berlin, 1987, p. 250.
- [8] J.E. Martin, J.P. Wilcoxon, J. Odinek, Phys. Rev. A 43 (1991) 858.
- [9] S.Z. Ren, C.M. Sorensen, Phys. Rev. Lett. 70 (1993) 1727.
- [10] J.E. Martin, J.P. Wilcoxon, Phys. Rev. Lett. 61 (1988) 373.
- [11] S.Z. Ren, W.F. Shi, W.B. Zhang, C.M. Sorensen, Phys. Rev. A 45 (1992) 2416.
- [12] F. Bordi, C. Cametti, J. Rouch, F. Sciortino, P. Tartaglia J. Phys. Cond. Matt. 8 (1996) A19.
- [13] T. Hanai, in: P. Sherman (Ed.), Emulsion Science, Academic Press, New York, 1968.
- [14] M. Lagües, J. Phys. (Paris) Lett. 40 (1979) L331.
- [15] G.S. Grest, I. Webman, S. Safran, A.L.R. Bug, Phys. Rev. A 33 (1986) 2842.
- [16] F. Bordi, C. Cametti, P. Codastefano, F. Sciortino, P. Tartaglia, J. Rouch, Progress in Colloid and Polymer Science, Steinkopff Verlag, Darmstadt, 1996.
- [17] C. Cametti, P. Codastefano, A. Di Biasio, P. Tartaglia, S.H. Chen, Phys. Rev. A 40 (1989) 1962.
- [18] W. Götze, L. Sjögren, Rep. Prog. Phys. 55 (1992) 241.
- [19] W. Götze, L. Sjögren, Transport Theory and Statistical Physics 24 (1995) 801.
- [20] T. Odagaki, Phys. Rev. Lett. 75 (1995) 3701.
- [21] P. Gallo, F. Sciortino, P. Tartaglia, S.H. Chen, Phys. Rev. Lett. 76 (1996) 2730.
- [22] F. Sciortino, P. Gallo, P. Tartaglia, S.H. Chen, Phys. Rev. E54 (1996) 6331.